

3,4-Disubstituted Polyalkylthiophenes for High-Performance Thin-Film Transistors and Photovoltaics

Sangwon Ko,[†] Eric Verploegen,^{‡,§} Sanghyun Hong,[‡] Rajib Mondal,[‡] Eric T. Hoke,[⊥] Michael F. Toney,[§] Michael D. McGehee,^{||} and Zhenan Bao^{*,‡}

Departments of [†]Chemistry, [‡]Chemical Engineering, [⊥]Applied Physics, and ^{||}Materials Science and Engineering, Stanford University, Stanford, California 94305, United States

[§]Stanford Synchrotron Radiation Lightsource, Menlo Park, California 94025, United States

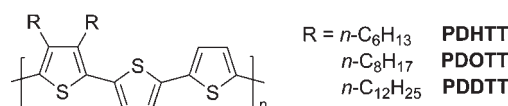
S Supporting Information

ABSTRACT: We demonstrate that poly(3,4-dialkylterthiophenes) (P34ATs) have comparable transistor mobilities ($0.17 \text{ cm}^2 \text{ V}^{-1} \text{ s}^{-1}$) and greater environmental stability (less degradation of on/off ratio) than regioregular poly(3-alkylthiophenes) (P3ATs). Unlike poly(3-hexylthiophene) (P3HT), P34ATs do not show a strong and distinct π - π stacking in X-ray diffraction. This suggests that a strong π - π stacking is not always necessary for high charge-carrier mobility and that other potential polymer packing motifs in addition to the edge-on structure (π - π stacking direction parallel to the substrate) can lead to a high carrier mobility. The high charge-carrier mobilities of the hexyl and octyl-substituted P34AT produce power conversion efficiencies of 4.2% in polymer:fullerene bulk heterojunction photovoltaic devices. An enhanced open-circuit voltage (0.716–0.771 eV) in P34AT solar cells relative to P3HT due to increased ionization potentials was observed.

The advantages of easy fabrication, low cost, and compatibility with flexible and lightweight plastic substrates have promoted the development of many promising semiconducting polymers.^{1–4} Poly(3-hexylthiophene) (P3HT) has been the most studied organic semiconductor for solution-processable thin-film transistors and organic solar cells.^{5,6} Regioregular P3HT has a coplanar rigid polymer backbone that facilitates the formation of a lamellar packing structure in thin films. The highly delocalized π conjugation along the polymer backbone and a strong π - π interchain stacking results in a high field-effect mobility (0.05 – $0.2 \text{ cm}^2 \text{ V}^{-1} \text{ s}^{-1}$).^{7–9} Regioregular P3HT-based bulk heterojunction (BHJ) solar cells with [6,6]-phenyl- C_{61} -butyric acid methyl ester (PC_{61}BM) have power conversion efficiencies (PCEs) of >4%.^{6,10} The high charge transport in P3HT enables the device to be made thicker ($\sim 220 \text{ nm}$) than most other polymer–fullerene devices, which allows for greater reproducibility in manufacturing.

In small-molecule semiconductors, the packing structure plays an important role in controlling charge transport.¹¹ Because of their monodispersity and high crystallinity, the packing structures have been intensively studied to correlate the packing motif with the carrier mobility. One effective way to vary the packing motif is to functionalize aromatic rings with substituents. For example, the herringbone packing structure of acenes can be

Scheme 1. Molecular Structures of PDHTT, PDOTT, and PDDTT



changed to a face-to-face packing structure by choosing the proper substituents.^{12–15} On the other hand, for polymers, it is usually hard to form highly ordered arrangements because of their high molecular weights and polydispersities. Good charge transport is usually observed with polymers having an edge-on conformation and forming lamellar structures with a strong π - π stacking. The strong π - π stacking of the planar polymer backbone has been a key structural feature of many semicrystalline semiconductors with high charge-carrier mobility, leading to intensive studies of materials containing 3-alkylthiophene building blocks.^{16–21}

In this communication, we report charge-carrier mobilities of up to $0.17 \text{ cm}^2 \text{ V}^{-1} \text{ s}^{-1}$ for films annealed above their melting temperatures (T_m) and unannealed solar cell PCEs of up to 4.2% for poly(3,4-dialkylterthiophenes) (P34ATs). Previous reports have described the synthesis (via oxidative polymerization) and optical properties of poly(3,4-dihexyl-2,2'-bithiophene)²² and poly(3,4-dihexyl-2,2':5',2''-terthiophene).²³ It was reported that these polymers showed poor ordering, which was attributed to steric hindrance between the dialkyl chains and adjacent thiophene rings that created torsion along the polymer backbone. However, we found that with the proper selection of comonomer, P34ATs form further ordered structures after thermal annealing above T_m , resulting in high charge-carrier mobilities and solar cell efficiencies comparable to or in some cases exceeding those of poly(3-alkylthiophene) (P3AT) devices.^{24,25} Interestingly, a strong π - π stacking peak was not observed in the P34AT thin films despite the high charge-carrier mobility. P34AT transistor devices additionally exhibited greater stability in the on/off ratio under ambient conditions than P3HT devices because of the larger ionization potentials (IPs) of P34ATs. We also found that incorporation of the 3,4-dialkylthiophene is a versatile method for tuning the packing structure of the corresponding polymer, since comonomers can be easily varied for

Received: April 5, 2011

Published: October 05, 2011

Table 1. Number-Average Molecular Weights (M_n), Polydispersity Indexes (PDI), Optical Band Gaps (E_g^{opt}), and Ionization Potentials (IP) for P34ATs

polymer	M_n (kDa)	PDI	λ_{max}	E_g^{opt} (eV) ^a	IP (eV) ^b
PDHHT	8.6	1.5	510	1.96	5.15
PDO TT	15	1.6	518	1.97	5.14
PDDTT	22	1.8	518	1.99	5.17

^a Estimated from the onset of the absorption spectrum. ^b Determined by CV of thin films.

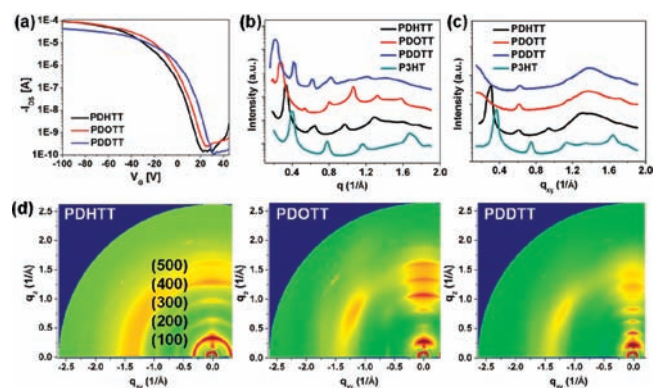


Figure 1. (a) Representative transfer curves for TFTs fabricated with PDHHT, PDO TT, and PDDTT tested under an inert atmosphere ($V_D = -100$ V). (b) Out-of-plane GIXS curves for films of PDHHT, PDO TT, PDDTT, and P3HT (annealed above T_m). These curves were taken from a slice in the direction perpendicular to the substrate. (c) In-plane GIXS curves. (d) 2D GIXS images.

Stille polymerization with a 3,4-dialkylthiophene. This may open up new opportunities for tuning polymer electronic properties.

Three P34ATs (PDHHT, PDO TT, and PDDTT) having alkyl substituents (*n*-hexyl, *n*-octyl, and *n*-dodecyl, respectively) at the 3 and 4 positions of thiophene with bithiophene spacers (Scheme 1) were synthesized from Stille polymerizations [see the Supporting Information (SI)]. The optical band gaps (E_g^{opt}) of the P34ATs in films are very similar to each other (1.96–1.99 eV; Table 1), but the absorption maxima are blue-shifted by ~ 40 nm relative to P3HT ($E_g^{\text{opt}} = 1.90$ eV), likely as a result of increased twisting of the conjugated backbone in the P34AT thin films (Figure S1 in the SI). The IPs of the polymers (5.15, 5.14, and 5.17 eV for PDHHT, PDO TT, and PDDTT, respectively; Table 1) all are higher than that of P3HT (4.99 eV), as measured by cyclic voltammetry (CV) of the thin films (Figure S1). This is attributed to the lower average number of electron-donating alkyl chain substituents per thiophene ring ($2/3$) than in P3HT (1), which has previously been shown to increase the IP in other poly(alkylthiophenes).²⁶

According to thermogravimetric analysis (TGA), these polymers have high thermal stability (>400 °C) under nitrogen (Figure S2). The melting points ($T_m = 201$, 193, and 178 °C for PDHHT, PDO TT, and PDDTT, respectively) were measured using differential scanning calorimetry (DSC) and found to decrease with increasing alkyl chain length (Figure S2).^{27,28}

The charge-transport properties of the spin-coated polymer films were evaluated using bottom-gate, top-contact field-effect transistors (FETs) built on *n*-doped SiO_2 (300 nm)/Si wafers

Table 2. Results for Top-Contact FETs ($W/L = 20$, $L = 50$ μm) Tested under an Inert Atmosphere after Annealing above T_m ^a

polymer	T_{anneal} (°C)	μ_{avg} ($\text{cm}^2 \text{V}^{-1} \text{s}^{-1}$)	on/off ratio	V_T (V)
PDHHT	210	0.12 ± 0.03	10^5 – 10^6	5.2 ± 3.0
PDO TT	205	0.12 ± 0.04	10^5 – 10^6	2.7 ± 4.6
PDDTT	185	0.10 ± 0.03	10^4 – 10^5	17.9 ± 1.5

^a From tests on at least 10 devices.

modified with a crystalline octadecyltrimethoxysilane (OTS-Y) monolayer.²⁹ Representative I – V transfer curves tested under an inert atmosphere are shown in Figure 1a, and Table 2 summarizes the average transistor characteristics of all the polymers after annealing above T_m . After the films were annealed at 80 °C, the initial mobilities (μ) were 0.020, 0.027, and 0.030 $\text{cm}^2 \text{V}^{-1} \text{s}^{-1}$ for PDHHT, PDO TT, and PDDTT, respectively, with on/off ratios on the order of 10^4 – 10^5 (Table S1 in the SI). These values are similar to those previously reported for other P34ATs.³⁰ After the films were annealed above T_m (185–210 °C), the devices gave improved average μ values of 0.12, 0.12, and 0.10 $\text{cm}^2 \text{V}^{-1} \text{s}^{-1}$, respectively, with on/off ratios of 10^5 – 10^6 (Table 2). The average threshold voltages (V_T) were 5.2, 2.7, and 17.9 V, respectively. As shown in Table 2, P34AT thin-film transistor (TFT) mobilities are not significantly affected by variation of the alkyl chain.

As observed by atomic force microscopy (AFM) (Figure S3), the thin films of the polymers developed oriented, nodular-shaped nanocrystalline domains when annealed above T_m . The interlayer lamellar $d(100)$ spacings and π – π stacking distances in the films of the P34ATs were determined by grazing-incidence X-ray scattering (GIXS). Intense diffraction with several high-order ($n00$) peaks was observed along the nominally out-of-plane (q_z) direction for PDHHT, PDO TT, and PDDTT films annealed above T_m , with lamellar d spacings of 19.0, 23.0, and 29.2 Å, respectively (Figure 1b,d). In comparison with P3HT (15.9 Å), PDHHT shows a larger d spacing (19.0 Å). Larger lamellar d spacings were also observed for PDO TT (23.0 Å) compared with P3OT (20.1 Å) and PDDTT (29.0 Å) compared with P3DDT (27.2 Å).²⁸ These ($n00$) peaks from P34AT films annealed above T_m are more distinct than those for films annealed at 80 °C (Figure S4), indicating more ordered structures on films annealed above T_m .

Despite exhibiting mobilities similar to those of P3ATs,²⁴ the P34ATs showed very weak π – π stacking in comparison with P3HT ($q_{xy} = 1.64 \text{ \AA}^{-1}$, π – π stacking distance = 3.83 Å) (Figure 1c). The in-plane scattering intensity from π – π stacking of P34ATs (near $q_{xy} = 1.72 \text{ \AA}^{-1}$, π – π stacking distance ≈ 3.65 Å) is at least 9 times lower than that from the P3HT film. Therefore, they are too weak to be analyzed quantitatively beyond determining the peak position. This suggests that strong π – π stacking is not always necessary for achieving high carrier mobilities. The reduced π – π stacking distance (~ 3.65 Å) could be partially responsible for the good mobilities. However, the intensity from π – π stacking is so low for the P34ATs that it is hard to attribute the good mobilities to this alone. For amorphous triarylamine copolymer transistors, a mobility of up to 0.04 $\text{cm}^2 \text{V}^{-1} \text{s}^{-1}$ has been reported.³¹ Poly(2,5-bis(3-alkyl-5-(3-alkylthiophen-2-yl)thiophen-2-yl)thiazolo[5,4-*d*]thiazole (PTzQT) polymers having isotropic amorphous-like superstructures in films have shown mobilities of $>0.1 \text{ cm}^2 \text{V}^{-1} \text{s}^{-1}$.³² In addition, a mobility

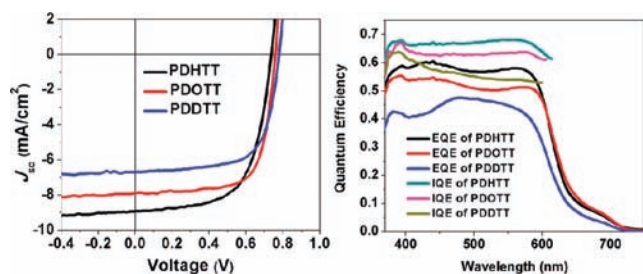


Figure 2. J – V curves and quantum efficiencies of polymer solar cells based on PDHTT, PDOTT, and PDDTT under illumination with AM 1.5G solar simulated light ($100 \text{ mW}/\text{cm}^2$).

Table 3. Photovoltaic Properties of Polymer Solar Cells Blended with $\text{PC}_{71}\text{BM}^a$

polymer	μ_h ($\text{cm}^2 \text{V}^{-1} \text{s}^{-1}$)	J_{sc} (mA/cm^2)	V_{oc} (V)	FF	PCE (PCE_{max}) (%)
P3HT	3×10^{-4}	8.95	0.604	0.69	3.74 (3.96) ^b
PDHTT	3×10^{-4}	8.54	0.716	0.66	4.01 (4.20)
PDOTT	2×10^{-4}	7.96	0.754	0.67	4.03 (4.23) ^b
PDDTT	3×10^{-5}	6.42	0.771	0.65	3.23 (3.53) ^b

^a Optimum devices were fabricated with polymer: PC_{71}BM = 1:0.8 for PDHTT and PDDTT and 1:1 for P3HT and PDOTT; results are based on tests of at least seven devices. ^b Annealed at 110°C for 10 min.

of $0.18 \text{ cm}^2 \text{V}^{-1} \text{s}^{-1}$ was observed in the face-on packing of the n-type polymer poly{[N,N' -bis(2-octyldodecyl)naphthalene-1,4,5,8-bis(dicarboximide)-2,6-diyl]-alt-5,5'-(2,2'-bithiophene)} [P(NDIOD-T2)].³³ We suggest that interdomain (grain) connectivity in P34ATs may account for the high mobility, which would indicate that its charge transport is three-dimensional. The noticeably larger lamellar d spacings of P34ATs relative to the corresponding P3ATs^{18,28,32} and the extremely weak π – π stacking suggest that the P34AT polymer backbones are less ordered. However, the weaker π – π stacking makes it less likely to form the nanofibrillar structures typically observed in polymers with 3-alkylthiophenes^{34,35} and promote better connectivity between grains as shown in AFM images (Figure S3). The less anisotropic morphology (nodular-shaped grains) may provide electronic pathways across grain boundaries and reduce the associated transport barrier.^{35,36}

Although the exact solid-state structures of P34ATs are yet to be solved, the distinct longer lamellar d spacings than in P3ATs and the weak π – π stacking of the P34ATs suggest that P34ATs do not have the same commonly observed edge-on structure (π – π stacking direction parallel to the substrate). However, high charge-carrier mobilities can still be obtained.

Consistent with their higher IPs, devices fabricated from P34ATs showed higher environmental stability (i.e., less degradation of the on/off ratio) than those from P3HT. After being stored under ambient conditions in the dark for 30 days ($\sim 55\%$ humidity), the devices showed only slightly decreased mobilities of 0.080 , 0.069 , and $0.062 \text{ cm}^2 \text{V}^{-1} \text{s}^{-1}$ for PDHTT, PDOTT, and PDDTT, respectively, with on/off ratios of $\sim 10^5$. This is in sharp contrast to the drastic degradation in on/off ratio ($\sim 10^2$) of regioregular P3HT devices under ambient conditions (Table S2 and Figure S5).

The photovoltaic properties of the P34ATs were investigated in the device structure ITO/PEDOT:PSS/polymer:PCBM/Ca/Al.

In the optimized devices, the active layers were spin-cast from chlorobenzene for PDHTT and PDOTT and from 1,2-dichlorobenzene for PDDTT. The best current density–voltage (J – V) curves are shown in Figure 2, and the average device characteristics are summarized in Table 3. For comparison, solar cells based on P3HT were fabricated following reported optimized procedures,⁶ and PCEs of 3.76 and 3.96% with PC_{61}BM and PC_{71}BM were obtained after thermal annealing (Table S3). For the optimized devices from PDHTT, PDOTT, and PDDTT with PC_{71}BM , we obtained PCEs of 4.20, 4.23, and 3.53%, respectively. Interestingly, thermal annealing did not much change the measured PCE for PDHTT (Table S3), and it should be noted that neither thermal annealing nor the use of a slow-drying solvent was required for PDHTT devices to obtain a PCE of 4.2%. Furthermore, a PCE of 3.83% could be obtained for PDHTT devices up to 197 nm in thickness (Table S3). This is important because thicker films are desirable for uniform coating over a large area. Comparison of the short-circuit current densities (J_{sc}) (Table 3) showed that the devices based on PDDTT gave lower J_{sc} values (8.54, 7.96, and $6.42 \text{ mA}/\text{cm}^2$ for PDHTT, PDOTT, and PDDTT, respectively), which is attributed to the lower hole mobilities with increasing alkyl chain length, as observed from hole-only space-charge-limited current (SCLC) diode mobility measurements (Table 3). The SCLC hole mobilities for P34AT: PC_{71}BM blends were measured using a ITO/PEDOT:PSS/polymer: PC_{71}BM /Au device structure. The SCLC diode mobilities of PDHTT and PDOTT (3×10^{-4} and $2 \times 10^{-4} \text{ cm}^2 \text{V}^{-1} \text{s}^{-1}$) are comparable to that of P3HT ($3 \times 10^{-4} \text{ cm}^2 \text{V}^{-1} \text{s}^{-1}$), while the mobility of PDDTT ($3 \times 10^{-5} \text{ cm}^2 \text{V}^{-1} \text{s}^{-1}$) is an order of magnitude lower than those of PDHTT and PDOTT. External and internal quantum efficiency spectra also confirmed better charge collection in solar cells based on PDHTT, which contains shorter alkyl chains (Figure 2). The open-circuit voltages (V_{oc}) for the P34ATs-based solar cells were in the range 0.716–0.771 V, which is 0.1–0.2 V higher than for P3HT solar cells (Table 3) because of the higher IPs. The P34AT solar cells exhibited fill factors (FF) in the range 0.65–0.67, which is comparable to that of P3HT devices. The moderate FF for PDDTT can be achieved in spite of low diode mobility due to the use of a thin device (Table S3).

In summary, we have shown that poly(3,4-dialkylterthiophenes) have comparable transistor and photovoltaic performance but greater environmental stability in on/off ratio than regioregular P3AT polymers. A weak π – π stacking was observed for these polymers, suggesting that a strong π – π stacking is not always essential for high performance in electronic devices. This work also suggests that the lower degree of order of the conjugated backbones may facilitate connectivity between grains. The observed mobility is a combination of intra- and intergrain mobility. The intragrain mobility may be decreased in P34ATs as a result of the less ordered packing; however, the intergrain transport is enhanced by good intergrain connectivity. Therefore, the net result can lead to mobilities comparable to those in P3HT-based devices. Although the exact packing motif of P34AT has not yet been resolved, other potential polymer packing motifs in addition to the commonly seen edge-on structure can lead to a high carrier mobility. Modeling combined with experiments to elucidate the structures of the various P34ATs is ongoing.

■ ASSOCIATED CONTENT

S Supporting Information. Experimental details; synthesis of the monomers and polymers; device preparations and characterizations; UV, CV, TGA, DSC, and GIXS plots; AFM images; and optimization of FET and photovoltaic properties. This material is available free of charge via the Internet at <http://pubs.acs.org>.

■ AUTHOR INFORMATION

Corresponding Author

zbao@stanford.edu

■ ACKNOWLEDGMENT

This publication was partially based on work supported by the Center for Advanced Molecular Photovoltaics, Award KUS-C1-015-21, made by King Abdullah University of Science and Technology (KAUST). Portions of this research were carried out at the Stanford Synchrotron Radiation Lightsources User Facility operated by Stanford University on behalf of the U.S. Department of Energy, Office of Basic Energy Sciences.

■ REFERENCES

- (1) Garnier, F.; Hajlaoui, R.; Yassar, A.; Srivastava, P. *Science* **1994**, *265*, 1684.
- (2) Dimitrakopoulos, C. D.; Purushothaman, S.; Kymissis, J.; Callegari, A.; Shaw, J. M. *Science* **1999**, *283*, 822.
- (3) Bao, Z. N. *Adv. Mater.* **2000**, *12*, 227.
- (4) Gelinck, G. H.; Geuns, T. C. T.; de Leeuw, D. M. *Appl. Phys. Lett.* **2000**, *77*, 1487.
- (5) Sirringhaus, H.; Tessler, N.; Friend, R. H. *Science* **1998**, *280*, 1741.
- (6) Li, G.; Shrotriya, V.; Huang, J. S.; Yao, Y.; Moriarty, T.; Emery, K.; Yang, Y. *Nat. Mater.* **2005**, *4*, 864.
- (7) Sirringhaus, H.; Brown, P. J.; Friend, R. H.; Nielsen, M. M.; Bechgaard, K.; Langeveld-Voss, B. M. W.; Spiering, A. J. H.; Janssen, R. A. J.; Meijer, E. W.; Herwig, P.; de Leeuw, D. M. *Nature* **1999**, *401*, 685.
- (8) Wang, G. M.; Swensen, J.; Moses, D.; Heeger, A. J. *J. Appl. Phys.* **2003**, *93*, 6137.
- (9) Bao, Z.; Dodabalapur, A.; Lovinger, A. J. *Appl. Phys. Lett.* **1996**, *69*, 4108.
- (10) Dennler, G.; Scharber, M. C.; Brabec, C. J. *Adv. Mater.* **2009**, *21*, 1323.
- (11) Murphy, A. R.; Fréchet, J. M. J. *Chem. Rev.* **2007**, *107*, 1066.
- (12) Mattheus, C. C.; de Wijs, G. A.; de Groot, R. A.; Palstra, T. T. M. *J. Am. Chem. Soc.* **2003**, *125*, 6323.
- (13) Park, S. K.; Jackson, T. N.; Anthony, J. E.; Mourey, D. A. *Appl. Phys. Lett.* **2007**, *91*, No. 063514.
- (14) Moon, H.; Zeis, R.; Borkent, E. J.; Besnard, C.; Lovinger, A. J.; Siegrist, T.; Kloc, C.; Bao, Z. N. *J. Am. Chem. Soc.* **2004**, *126*, 15322.
- (15) Tang, M. L.; Reichardt, A. D.; Wei, P.; Bao, Z. N. *J. Am. Chem. Soc.* **2009**, *131*, 5264.
- (16) Ong, B. S.; Wu, Y. L.; Liu, P.; Gardner, S. J. *J. Am. Chem. Soc.* **2004**, *126*, 3378.
- (17) Heeney, M.; Bailey, C.; Genevicius, K.; Shkunov, M.; Sparrowe, D.; Tierney, S.; McCulloch, I. J. *J. Am. Chem. Soc.* **2005**, *127*, 1078.
- (18) McCulloch, I.; Heeney, M.; Bailey, C.; Genevicius, K.; MacDonald, I.; Shkunov, M.; Sparrowe, D.; Tierney, S.; Wagner, R.; Zhang, W. M.; Chabinyc, M. L.; Kline, R. J.; McGehee, M. D.; Toney, M. F. *Nat. Mater.* **2006**, *5*, 328.
- (19) Fong, H. H.; Pozdin, V. A.; Amassian, A.; Malliaras, G. G.; Smilgies, D. M.; He, M. Q.; Gasper, S.; Zhang, F.; Sorensen, M. *J. Am. Chem. Soc.* **2008**, *130*, 13202.
- (20) Osaka, I.; Abe, T.; Shinamura, S.; Miyazaki, E.; Takimiya, K. *J. Am. Chem. Soc.* **2010**, *132*, 5000.
- (21) Pan, H. L.; Li, Y. N.; Wu, Y. L.; Liu, P.; Ong, B. S.; Zhu, S. P.; Xu, G. *J. Am. Chem. Soc.* **2007**, *129*, 4112.
- (22) Andreani, F.; Salatelli, E.; Lanzi, M.; Bertinelli, F.; Fichera, A. M.; Gazzano, M. *Polymer* **2000**, *41*, 3147.
- (23) Belletete, M.; Mazerolle, L.; Desrosiers, N.; Leclerc, M.; Durocher, G. *Macromolecules* **1995**, *28*, 8587.
- (24) Sauve, G.; Javier, A. E.; Zhang, R.; Liu, J. Y.; Sydlík, S. A.; Kowalewski, T.; McCullough, R. D. *J. Mater. Chem.* **2010**, *20*, 3195.
- (25) Nguyen, L. H.; Hoppe, H.; Erb, T.; Gunes, S.; Gobsch, G.; Sariciftci, N. S. *Adv. Funct. Mater.* **2007**, *17*, 1071.
- (26) Hou, J. H.; Chen, T. L.; Zhang, S. Q.; Huo, L. J.; Sista, S.; Yang, Y. *Macromolecules* **2009**, *42*, 9217.
- (27) Park, Y. D.; Kim, D. H.; Jang, Y.; Cho, J. H.; Hwang, M.; Lee, H. S.; Lim, J. A.; Cho, K. *Org. Electron.* **2006**, *7*, 514.
- (28) Chen, T. A.; Wu, X. M.; Rieke, R. D. *J. Am. Chem. Soc.* **1995**, *117*, 233.
- (29) Ito, Y.; Virkar, A. A.; Mannsfeld, S.; Oh, J. H.; Toney, M.; Locklin, J.; Bao, Z. A. *J. Am. Chem. Soc.* **2009**, *131*, 9396.
- (30) Ong, B.; Wu, Y. L.; Jiang, L.; Liu, P.; Murti, K. *Synth. Met.* **2004**, *142*, 49.
- (31) Zhang, W. M.; Smith, J.; Hamilton, R.; Heeney, M.; Kirkpatrick, J.; Song, K.; Watkins, S. E.; Anthopoulos, T.; McCulloch, I. J. *J. Am. Chem. Soc.* **2009**, *131*, 10814.
- (32) Osaka, I.; Zhang, R.; Sauve, G.; Smilgies, D. M.; Kowalewski, T.; McCullough, R. D. *J. Am. Chem. Soc.* **2009**, *131*, 2521.
- (33) Rivnay, J.; Toney, M. F.; Zheng, Y.; Kauvar, I. V.; Chen, Z. H.; Wagner, V.; Facchetti, A.; Salleo, A. *Adv. Mater.* **2010**, *22*, 4359.
- (34) Kowalewski, T.; Zhang, R.; Li, B.; Iovu, M. C.; Jeffries-EL, M.; Sauve, G.; Cooper, J.; Jia, S. J.; Tristram-Nagle, S.; Smilgies, D. M.; Lambeth, D. N.; McCullough, R. D. *J. Am. Chem. Soc.* **2006**, *128*, 3480.
- (35) Salleo, A.; Kline, R. J.; DeLongchamp, D. M.; Chabinyc, M. L. *Adv. Mater.* **2010**, *22*, 3812.
- (36) McGehee, M. D.; Kline, R. J.; Kadnikova, E. N.; Liu, J. S.; Fréchet, J. M. J. *Adv. Mater.* **2003**, *15*, 1519.